ISET Journal of Earthquake Technology, Paper No. 587, Vol. 61, No. 3, Sept. 2024, pp. 71–90

A RESPONSE SPECTRUM-BASED MODAL COMBINATION RULE FOR PEAK SEISMIC RESPONSE USING PEAK FACTORS

Abhilash S. Ghumadwar
Department of Civil Engineering, Indian Institute of Technology Kanpur
Kanpur 208016, E mail id: *abilas124@gmail.com*

Vinay K. Gupta (Corresponding Author)
Department of Civil Engineering, Indian Institute of Technology Kanpur
Kanpur 208016, E mail id: *vinaykg@iitk.ac.in*

ABSTRACT

Most response spectrum-based modal combination rules used to estimate linear peak responses of multi-degree-of-freedom systems to specified seismic hazard assume that the nonstationary peak factors relating the root-mean-square responses to the largest response peaks are identical for the modal and overall system responses. This study accounts for the role of nonstationary peak factors by modifying an existing modal combination rule (a) which has been formulated for the peak value of an overall system response that can be expressed as a linear combination of the floor displacements in a lumped mass, classically damped, multistoried structure, and (b) which uses the hazard-consistent response spectrum ordinates to account for modal cross-correlation. To this end, available models for the normalized peak factors of the relative displacement and relative velocity responses of a base-excited single-degree-of-freedom system (where normalization is with respect to the peak factor for ground acceleration) are used. Also, the normalized peak factor for overall system response is modelled in terms of the normalized peak factors for modal responses. The proposed rule is illustrated in the case of floor displacement and story shear responses with the help of five buildings and six earthquake excitations in comparison with the existing modal combination rules.

KEYWORDS: Modal Combination Rule; Ground Acceleration Peak Factor; Relative Displacement Peak Factor; Relative Velocity Peak Factor; Overall Response Peak Factor; Normalized Peak Factor Models

INTRODUCTION

It is considered acceptable and convenient in the case of multi-degree-of-freedom (MDOF) systems to estimate the largest (elastic) peak response by using the response spectrum-based modal combination rules. These rules attempt to estimate the overall maximum of the desired response in terms of its modal maxima, which occur at different instants of time in response to a given ground motion. Starting from the sum of absolute modal maxima (SUM) method by Biot (1943), several attempts have been made to suitably combine the modal maxima of the desired response, e.g., the square-root-of-the-sum-of-the-squares (SRSS) method by Goodman et al. (1955), grouping and ten percent methods by USNRC (1976), complete-quadratic-combination (CQC) method by Wilson et al. (1981), modified CQC method by Der Kiureghian and Nakamura (1993), and complete-SRSS (CSRSS) method by Heredia-Zavoni (2011).

The basic differences in various modal combination rules relate to how modal cross-correlation arising from the close spacing of modes as well as from modes being stiff to the ground motion has been accounted for. The SUM method of Biot (1943) assumed various modal responses to be perfectly correlated on one extreme, while the SRSS method of Goodman et al. (1955) assumed those to be completely uncorrelated on the another extreme. Jennings (1958), Merchant and Hudson (1962), and O'Hara and Cunnif (1963) attempted to reduce the non-conservatism of the SRSS estimates by appropriately combining the SUM and SRSS methods. Rosenblueth and Elorduy (1969) were the first to account for modal cross-correlation in closely spaced modes without adopting any ad hoc measures and by formulating correlation coefficients for the responses in different pairs of modes. USNRC (1976) proposed the grouping and ten percent methods by assuming the responses in closely spaced modes to be fully correlated and the responses in the remaining modes and various groups of closely spaced modes to be uncorrelated. The CQC method by Der Kiureghian (1981) and Wilson et al. (1981) accounted for the

modal cross-correlation in closely spaced modes through correlation coefficients formulated by using stationary random vibration theory. Lindley and Yow (1980) considered the stiff or high-frequency modes to be fully correlated with each other and the remaining modes to be uncorrelated with each other and with the high-frequency modes. Singh and Mehta (1983) accounted for both types of modal cross-correlation (due to the close spacing of modes as well as due to the modes being stiff to the ground motion) by proposing two formulations: one based on the mode displacement approach and another based on the mode acceleration approach. Their mode acceleration formulation enabled the truncation of significant high-frequency modes without involving any 'missing-mass effect'. Gupta (1990) provided a heuristic solution to the problem of correlation between high-frequency modes by (a) considering each modal response to be composed of rigid and damped periodic parts, (b) by considering the rigid parts of different modes to be fully correlated, and (c) by accounting for the correlation between the damped periodic parts of different modes as in the CQC method. Singh and Maldonado (1991) modified the mode acceleration formulation of Singh and Mehta (1983) by considering the pseudo-static response in high-frequency modes and by using the approach of Anagnostopoulos (1982) to obviate the need of relative acceleration spectra consistent with the specified seismic hazard. Der Kiureghian and Nakamura (1993) followed a similar approach, but they proposed the use of a first-order approximation of hazard-consistent power spectral density function (PSDF) instead of hazard-consistent spectral velocity (SV) ordinates in the calculation of correlation coefficients. Gupta (1996) proposed an alternative to the mode-displacement formulation of Singh and Mehta (1983) (requiring the hazard-consistent SV ordinates to account for modal cross-correlation), while using the partial fractions of the modal cross-correlation term in the PSDF of the response process as in Gupta and Trifunac (1990). Heredia-Zavoni (2011) proposed a formulation similar to that of Gupta (1996), wherein a hazard-consistent PSDF is needed to account for modal cross-correlation (through characteristic frequency). Detailed reviews of some of the above methods have been provided by Gupta (2018) and Chopra (2021).

Almost all the modal combination rules mentioned above consider the modal maxima to be estimated via response spectrum ordinates, and therefore those assume the peak factors to be identical for the modal and overall responses. Here, peak factor refers to the nonstationary peak factor, which is defined as the ratio of the largest peak value in the given nonstationary process to the root-mean-square (RMS) value of the process assumed to be a stationary process. As argued by Ghumadwar and Gupta (2025), a nonstationary peak factor is the product of stationary peak factor and nonstationarity factor. Whereas a stationary peak factor accounts for the scaling up of the RMS value to the largest peak value in the process assumed to be a stationary process, a nonstationarity factor accounts for the scaling up/down of the largest peak value in the stationary process to that in the given nonstationary process. Further, the nonstationarity factors of ground acceleration and response processes are different in that the nonstationarity factor of a response process also accounts for the nonstationarity factor due to the finite operating time of the excitation (besides accounting for the inherent nonstationarity in the ground acceleration). It has been shown by Pal and Gupta (2021a) and Ghumadwar and Gupta (2025) that for the special situation of absolute floor acceleration response being the overall system response, the estimates based on the assumption of identical peak factors in a modal combination rule can be significantly improved by duly accounting for the role of peak factors through the modelling of normalized peak factors (where normalization is with respect to the peak factor of ground acceleration process).

Most of the modal combination rules developed since the modified CQC rule by Der Kiureghian and Nakamura (1993) require the use of hazard-consistent PSDF to account for modal cross-correlation. Due to this, the simplicity and convenience of using response spectrum-based modal combination rules are compromised. However, as shown by Singh and Mehta (1983), Gupta (1990), Singh and Maldonado (1991), and Gupta (1996), it is possible to account for the modal cross-correlation without using hazard-consistent PSDF, provided the hazard-consistent SV ordinates can be reliably obtained from the specified PSA spectrum. The approximation of SV ordinates as pseudo spectral velocity (PSV) ordinates is considered acceptable only at the intermediate periods. This study considers the estimation of hazard-consistent SV ordinates as proposed by Gupta (2009), Samdaria and Gupta (2018), and Pal and Gupta (2021b).

In this study the response spectrum-based modal combination rule proposed by Gupta (1996) for the peak responses of lumped mass, classically damped, base-excited multistoried structures is modified to include the role of various (nonstationary) peak factors. This rule is only for those overall responses that can be expressed as the linear combinations of floor displacements. For the proposed modification, the normalized peak factors for the relative displacement and relative velocity responses of a base-excited

single-degree-of-freedom (SDOF) system (where normalization is with respect to the peak factor for ground acceleration) are modelled as in Pal and Gupta (2021a) and Ghumadwar and Gupta (2025), respectively. Also, an expression for the normalized peak factor for overall response is developed in terms of the known normalized peak factors for modal responses. Finally, a numerical study is carried out to illustrate the performance of the proposed modal combination rule vis-a-vis the existing modal combination rules in the case of floor displacement and story shear responses of five example buildings under six example seismic hazards.

PEAK FACTOR-BASED MODAL COMBINATION RULE

The largest peak r_{peak} in any response $r(t)$ of a classically damped, linear system with the lumped masses, m_1, m_2, …, m_n, to the seismic hazard characterized by a set of design spectra may be estimated conveniently by using a response-spectrum based modal combination rule. For the situation where the response $r(t)$ can be expressed as a linear combination of the floor displacements, this study considers the modal combination rule proposed by Gupta (1996) for the estimation of r_{peak}. When the normalized nonstationary peak factors for various responses (where normalization is with respect to the nonstationary peak factor for ground acceleration) are not assumed to be equal, the rule proposed by Gupta (1996) may be modified to

$$\bar{r}_{\text{peak}}^2 = \sum_{j=1}^{n}\left[\rho_j^2\alpha_j^2\left(\frac{\bar{p}_r}{\bar{p}_j^D}\right)^2 \text{SD}_j^2 + \sum_{k=1,k\neq j}^{n}\rho_j\rho_k\alpha_j\alpha_k\left\{\left(C_{jk}+D_{jk}\right)\left(\frac{\bar{p}_r}{\bar{p}_j^D}\right)^2\text{SD}_j^2 - D_{jk}\left(\frac{\bar{p}_r}{\bar{p}_j^V}\right)^2\frac{\text{SV}_j^2}{\omega_j^2}\right\}\right] \tag{1}$$

In this equation, ρ_j denotes the normalized amplitude of the response $r(t)$ in the jth mode. For example, if the response $r(t)$ denotes the relative displacement at the ith floor level or shear force in the ith story, ρ_j becomes equal to $\phi_i^{(j)}$ (for the displacement response) or $\omega_j^2\sum_{l=i}^{n}m_l\phi_l^{(j)}$ (for the shear force response). Further, ω_j, α_j, and $\phi_i^{(j)}$ respectively represent the natural frequency, modal participation factor, and ith element of the mode shape in the jth mode of the system; $\bar{p}_r$ represents the nonstationary peak factor p_r for the response process $r(t)$ after normalization with respect to the nonstationary peak factor p_G for the given ground acceleration process; $\bar{p}_j^D$ and $\bar{p}_j^V$ respectively represent the normalized versions of the nonstationary peak factors p_j^D and p_j^V for the relative displacement and relative velocity responses of the SDOF oscillator (of ω_j frequency and ζ_j damping ratio) which is excited by the given ground acceleration process at its base; and SD_j and SV_j respectively represent the spectral displacement (SD) and SV ordinates at the frequency ω_j corresponding to the specified design spectrum for the damping ratio ζ_j. Further, the coefficients C_{jk} and D_{jk} are expressed as

$$C_{jk} = \frac{1}{B_{jk}}\left[8\zeta_j(\zeta_j+\zeta_k\varrho)\left\{\left(1-\varrho^2\right)^2 - 4\varrho\left(\zeta_j-\zeta_k\varrho\right)\left(\zeta_k-\zeta_j\varrho\right)\right\}\right] \tag{2}$$

$$D_{jk} = \frac{1}{B_{jk}}\left[2\left(1-\varrho^2\right)\left\{4\varrho\left(\zeta_j-\zeta_k\varrho\right)\left(\zeta_k-\zeta_j\varrho\right) - \left(1-\varrho^2\right)^2\right\}\right] \tag{3}$$

$$B_{jk} = 8\varrho^2\left[\left(\zeta_j^2+\zeta_k^2\right)\left(1-\varrho^2\right)^2 - 2\left(\zeta_k^2-\zeta_j^2\varrho^2\right)\left(\zeta_j^2-\zeta_k^2\varrho^2\right)\right] + \left(1-\varrho^2\right)^4 \tag{4}$$

with $\varrho = \omega_k/\omega_j$.

It may be observed that when the normalized peak factors, $\bar{p}_r$, $\bar{p}_j^D$, and $\bar{p}_j^V$, are assumed to be equal, Equation (1) will give the conventional estimates of r_{peak}. Same estimates will be obtained by alternatively assuming the normalized peak factors to be equal to unity.

NORMALIZED PEAK FACTORS FOR MODAL RESPONSES

The response $\xi_j(t)$ of the modal (SDOF) oscillator in the jth mode (of ω_j frequency and ζ_j damping ratio), which is excited by the given ground acceleration $\ddot{z}(t)$ at its base, is governed by the following equation:

$$\ddot{\xi}_j(t) + 2\zeta_j\omega_j\dot{\xi}_j(t) + \omega_j^2\xi_j(t) = -\ddot{z}(t); \quad j = 1,2,...,n \tag{5}$$

where $\dot{\xi}_j(t)$ and $\ddot{\xi}_j(t)$ respectively denote the first and second derivatives of $\xi_j(t)$. Assuming the response $\xi_j(t)$ to be a stationary process, the PSDF $S_\xi(\omega)$ of this process is obtained from the PSDF of the ground acceleration process $S_{\ddot{z}}(\omega)$ as

$$S_\xi(\omega) = \left|H_\xi(\omega)\right|^2 S_{\ddot{z}}(\omega) \tag{6}$$

where

$$H_\xi(\omega) = \frac{-1}{\omega_j^2 - \omega^2 + 2i\zeta_j\omega_j\omega} \tag{7}$$

is the transfer function relating the response $\xi_j(t)$ to the input $\ddot{z}(t)$. Further, the PSDF $S_{\ddot{z}}(\omega)$ of the ground acceleration process is expressed in terms of the Fourier spectrum $\left|Z(\omega)\right|$ of ground acceleration $\ddot{z}(t)$ as

$$S_{\ddot{z}}(\omega) = \frac{E\left[\left|Z(\omega)\right|^2\right]}{\pi T_s} \tag{8}$$

where the expectation operator $E[.]$ may be applied via the smoothening of $\left|Z(\omega)\right|^2$ over frequency ω, and the strong-motion duration T_s of the $\ddot{z}(t)$ record may be assumed to denote the duration of the (stationary) ground acceleration process.

The nonstationary peak factor for the expected value of the largest peak in ground acceleration (= $\max_t |\ddot{z}(t)|$), i.e., PGA, is expressed as

$$p_G = \frac{\text{PGA}}{\ddot{z}_{\text{rms}}} \tag{9}$$

where $\ddot{z}_{\text{rms}}$ is the RMS value of the ground acceleration process. It is obtained from the PSDF $S_{\ddot{z}}(\omega)$ of the process (see Equation (8)), with strong-motion duration T_s assumed to be same as that defined by Trifunac and Brady (1975), by taking the square root of the area under $S_{\ddot{z}}(\omega)$. Further, the nonstationary peak factor for the expected value of the largest relative displacement response (= $\max_t |\xi_j(t)|$), i.e., SD_j is expressed as

$$p_j^D = \frac{\text{SD}_j}{\xi_{j,\text{rms}}} \tag{10}$$

where $\xi_{j,\text{rms}}$ denotes the RMS value of the relative displacement response. This is obtained by taking the square root of the area under the PSDF $S_\xi(\omega)$ defined in Equation (6). Similarly, the nonstationary peak factor for the expected value of the largest relative velocity response (= $\max_t |\dot{\xi}_j(t)|$), i.e., SV_j is expressed as

$$p_j^V = \frac{\text{SV}_j}{\dot{\xi}_{j,\text{rms}}} \tag{11}$$

where $\dot{\xi}_{j,\text{rms}}$ denotes the RMS value of the relative velocity response. This is obtained by taking the square root of the area under the corresponding PSDF $S_{\dot{\xi}}(\omega)$ (= $\omega^2 S_{\xi}(\omega)$).

On normalizing p_j^D and p_j^V by p_G, the normalized (nonstationary) peak factors $\bar{p}_j^D$ and $\bar{p}_j^V$ are obtained for the expected values of the largest relative displacement and relative velocity responses in the j th mode.

FORMULATION OF NORMALIZED PEAK FACTOR FOR OVERALL RESPONSE

The response $r(t)$ may be expressed in terms of the responses in different undamped modes of the system as

$$r(t) = \sum_{j=1}^{n} r_j(t) \tag{12}$$

with

$$r_j(t) = \alpha_j \rho_j \xi_j(t) \tag{13}$$

If the modal responses $r_j(t)$ and $r_k(t)$ in the j th and k th modes, respectively, are assumed to be statistically independent and the peak factors for the modal responses are assumed to be same as the peak factor for the response $r(t)$, the peak response r_{peak} may be expressed under the SRSS rule as

$$r_{\text{peak}} = \left[\sum_{j=1}^{n} r_{j,\text{peak}}^2 \right]^{\frac{1}{2}} \tag{14}$$

where

$$r_{j,\text{peak}} = \alpha_j \rho_j \text{SD}_j \tag{15}$$

represents the peak value of the modal response $r_j(t)$.

The peak value r_{peak} is also related to the RMS value r_{rms} of the response process $r(t)$ (which is estimated from the PSDF $S_{\ddot{z}}(\omega)$ of the ground acceleration process by using the stationary random vibration theory) through the nonstationary peak factor p_r as

$$r_{\text{peak}} = p_r r_{\text{rms}} \tag{16}$$

On ignoring the modal cross-correlation terms, the RMS value r_{rms} may be expressed as (Gupta, 1996)

$$r_{\text{rms}} = \left[\sum_{j=1}^{n} \left(\alpha_j \rho_j \frac{\text{SD}_j}{p_j^D} \right)^2 \right]^{\frac{1}{2}} \tag{17}$$

On using Equation (17) in Equation (16) and normalizing the peak factors, p_r and p_j^D, to $\bar{p}_r$ and $\bar{p}_j^D$, respectively, the peak response r_{peak} may be expressed as

$$r_{\text{peak}} = \bar{p}_r \left[\sum_{j=1}^{n} \left(\alpha_j \rho_j \frac{\text{SD}_j}{\bar{p}_j^D} \right)^2 \right]^{\frac{1}{2}} \tag{18}$$

Equation (15) is now substituted in Equation (14), and the so-obtained expression of the peak response r_{peak} is compared with that in Equation (18) to give the normalized peak factor $\bar{p}_r$ for the response process $r(t)$ as

$$\bar{p}_r = \left[\frac{\sum_{j=1}^{n} \left(\alpha_j \rho_j \text{SD}_j \right)^2}{\sum_{j=1}^{n} \left(\alpha_j \rho_j \text{SD}_j / \bar{p}_j^D \right)^2} \right]^{\frac{1}{2}} \tag{19}$$

Following a few manipulations, the preceding expression for $\bar{p}_r$ may alternatively be written as

$$\frac{1}{\bar{p}_r^2} = \sum_{j=1}^{n} \frac{w_j^2}{\left(\bar{p}_{r,j}\right)^2} \tag{20}$$

with

$$w_j^2 = \frac{\left(\alpha_j \rho_j \mathrm{SD}_j\right)^2}{\sum_{s=1}^{n} \left(\alpha_s \rho_s \mathrm{SD}_s\right)^2} \tag{21}$$

and

$$\bar{p}_{r,j} = \bar{p}_j^D \tag{22}$$

In Equations (20)–(22), the weight w_j is a measure of the relative contribution of the jth mode in the normalized peak factor $\bar{p}_r$ for the response process $r(t)$, and $\bar{p}_{r,j}$ denotes the normalized peak factor for the response process $r_j(t)$. It may be mentioned that the expression for the normalized peak factor $\bar{p}_r$ in the case of the displacement at the ith floor level (see Equations (20)–(22) with $\rho_j = \phi_i^{(j)}$) is similar to that of the normalized nonstationarity factor defined by Pathak and Gupta (2017).

The expression of the normalized peak factor $\bar{p}_r$ in Equation (20) is based on the assumptions that (a) when the modal cross-correlation is negligibly small, the SRSS approximation of the peak value of the response $r(t)$ is a reasonable approximation, and that (b) the normalized peak factor $\bar{p}_r$ is insensitive to the relative extent of modal cross-correlation in the RMS value of $r(t)$. These assumptions usually are not true, and hence Equation (20) may not give reliable estimates of the normalized peak factor $\bar{p}_r$. Therefore, a generalized form of Equation (20) is attempted in this study, wherein instead of the power of 2 on the weights and peak factors, a power of q is assumed, and the value of the parameter q is determined through calibration using the actual peak factors. Accordingly, the normalized peak factor $\bar{p}_r$ is considered as

$$\frac{1}{\bar{p}_r^q} = \sum_{j=1}^{n} \frac{w_j^q}{\left(\bar{p}_{r,j}\right)^q} \tag{23}$$

where the parameter q is determined for various types of responses with the help of a numerical exercise.

CALIBRATION OF PARAMETER q

1. Example Buildings and Excitations

As shown in a similar study by Pal and Gupta (2021a), the value of parameter q minimizing error between the actual and estimated responses (to a zero value most of the times) varies with the floor/story level, ground motion, and building considered. However, most of these values of q are around 2, and thus, it seems reasonable to consider a large range of building and ground motion combinations and to determine that value of q which minimizes the RMS error computed over all the floors/stories of the buildings in these combinations, for the modal combinations rule given in Equation (1). To this end, same 30 building and ground motion combinations are used as in Ghumadwar and Gupta (2025). These combinations correspond to six example ground motions listed in Table 1 and five example buildings. Three of the example buildings are symmetric, shear buildings with lumped masses and massless columns: (a) a 24-story building BD1 with a fundamental period of 2 s; (b) a 15-story building BD2 with a fundamental period of 1.2 s; and (c) a 5-story building BD3 with a fundamental period of 0.51 s. Table 2 gives the floor masses and story stiffnesses, and Table 3 gives the natural frequencies for these buildings. The remaining two example buildings are torsionally coupled shear buildings with massless columns and the centers of mass of different floors lying on one vertical axis: (a) a 7-story building BD4 with the dimensions of 20×25 m for the top four floors and 26×33 m for the bottom three floors, and

having a fundamental period of 0.5 s; and (b) a 15-story building BD5 with the dimensions of 25×100 m uniformly for all the floors, and having a fundamental period of 1.13 s. Tables 4 and 5 give the floor masses, radii of gyration (about the centres of mass), translational story stiffnesses in the x- and y-directions (which are aligned with the principal axes of resistance in the stories), torsional story stiffnesses, and eccentricities in the x- and y-directions for BD4 and BD5, respectively. Table 6 gives the natural frequencies of these buildings. All the five example buildings are assumed to be classically damped with 5%-damping in all the modes.

Table 1: Details of example ground motions considered

S. No.	Name of Earthquake	Recording Site Location	Comp.
1	1968 Borrego Mountain Earthquake	Engineering Building, Santa Ana, Orange County	S04E
2	1940 Imperial Valley Earthquake	El Centro, Imperial Valley Irrigation District	S00E
3	1952 Kern County Earthquake	Taft Lincoln School Tunnel	N21E
4	1966 Parkfield Earthquake	Array No. 5, Cholame, Shandon	N05W
5	1971 San Fernando Earthquake	Utilities Building, 215 West Broadway, Long Beach	N90E
6	1985 Michoacan earthquake	SCT Station, Mexico City	N90E

Table 2: Floor masses and story stiffnesses of example buildings BD1, BD2, and BD3

Floor Level	Floor Mass (t)			Story No.	Story Stiffness (kN/mm)		
	BD1	BD2	BD3		BD1	BD2	BD3
1	7426	280	166	**1**	6650	525	290
2	7426	200	166	**2**	6260	536	290
3	6918	200	166	**3**	5880	536	290
4	6970	200	166	**4**	5880	536	290
5	5849	200	141	**5**	5510	536	290
6	5587	200		**6**	5480	536	
7	5569	200		**7**	5480	536	
8	4063	200		**8**	5100	536	
9	3678	200		**9**	5010	536	
10	3678	200		**10**	5010	536	
11	3678	200		**11**	4960	536	
12	3415	200		**12**	4920	536	
13	3415	200		**13**	4920	536	
14	2855	200		**14**	4720	536	
15	2469	200		**15**	4670	536	
16	2469			**16**	4670		
17	2329			**17**	4610		
18	1769			**18**	4220		
19	1769			**19**	4220		
20	1524			**20**	4260		
21	1278			**21**	4240		
22	1261			**22**	4260		
23	928			**23**	4250		
24	771			**24**	4420		

Table 3: Natural frequencies of example buildings BD1, BD2, and BD3

Mode No.	Frequency (rad/s)		
	BD1	BD2	BD3
1	3.14	5.24	12.23
2	7.82	15.62	35.57
3	12.55	25.74	55.72
4	17.48	35.46	71.02
5	22.06	44.69	80.44

6	27.03	53.45	
7	31.25	61.79	
8	35.83	69.69	
9	39.84	77.04	
10	43.86	83.72	
11	47.66	89.57	
12	50.86	94.49	
13	54.15	98.40	
14	56.33	101.24	
15	58.88	102.96	
16	61.59		
17	66.06		
18	69.80		
19	72.86		
20	77.86		
21	83.24		
22	91.06		
23	103.23		
24	121.53		

Table 4: Floor masses, radii of gyration, translational and torsional story stiffnesses, and eccentricities of example building BD4

Floor Level	Floor Mass (t)	Radius of Gyration (m)	Story No.	Translational Stiffness (kN/mm)		Torsional Stiffness (kN-m/rad)	Eccentricities (m)	
				x-Dir	y-Dir		x-Dir	y-Dir
1	1150	12.015	**1**	5361	5229	1100×10^6	3.142	4.621
2	1150	12.015	**2**	5240	5083	1001×10^6	3.142	4.621
3	1150	12.015	**3**	4998	4792	948×10^6	3.142	4.621
4	800	9.242	**4**	3424	3112	278×10^6	2.218	2.403
5	800	9.242	**5**	3100	2697	242×10^6	1.848	2.403
6	800	9.242	**6**	2696	2179	197×10^6	1.848	2.403
7	800	9.242	**7**	2212	1392	144×10^6	1.848	2.403

Table 5: Floor masses, radii of gyration, translational and torsional story stiffnesses, and eccentricities of example building BD5

Floor Level	Floor Mass (t)	Radius of Gyration (m)	Story No.	Translational Stiffness (kN/mm)		Torsional Stiffness (kN-m/rad)	Eccentricities (m)	
				x-Dir	y-Dir		x-Dir	y-Dir
1	792	29.76	**1**	1971	2608	2950×10^6	2.976	2.976
2	768	29.76	**2**	1914	2391	2865×10^6	2.887	2.887
3	744	29.76	**3**	1857	2456	2779×10^6	2.827	2.827
4	721	29.76	**4**	1799	2381	2694×10^6	2.738	2.738
5	705	29.76	**5**	1742	2306	2608×10^6	2.649	2.649
6	681	29.76	**6**	1685	2229	2522×10^6	2.559	2.559
7	657	29.76	**7**	1628	2154	2437×10^6	2.470	2.470
8	634	29.76	**8**	1571	2077	2351×10^6	2.381	2.381
9	610	29.76	**9**	1514	2003	2266×10^6	2.292	2.292
10	586	29.76	**10**	1457	1928	2180×10^6	2.232	2.232
11	570	29.76	**11**	1399	1851	2095×10^6	2.143	2.143
12	546	29.76	**12**	1342	1776	2009×10^6	2.053	2.053
13	523	29.76	**13**	1285	1701	1924×10^6	1.964	1.964
14	499	29.76	**14**	1228	1624	1838×10^6	1.875	1.875
15	475	29.76	**15**	1183	1563	1770×10^6	1.786	1.786

Table 6: Natural frequencies of example buildings BD4 and BD5

Mode No.	Frequency (rad/s)		Mode No.	Frequency (rad/s)		Mode No.	Frequency (rad/s)
	BD4	BD5		BD4	BD5		BD5
1	12.51	5.55	**16**	100.66	57.13	**31**	96.63
2	14.63	6.32	**17**	108.52	59.48	**32**	96.11
3	18.85	7.34	**18**	113.35	60.14	**33**	97.66
4	29.26	15.08	**19**	122.42	67.64	**34**	97.81
5	35.00	17.19	**20**	129.37	68.48	**35**	98.41
6	42.71	19.91	**21**	156.85	68.93	**36**	102.91
7	45.86	24.75	**22**		74.52	**37**	106.38
8	55.83	28.26	**23**		77.26	**38**	106.94
9	63.22	32.66	**24**		79.41	**39**	109.84
10	67.50	34.18	**25**		80.59	**40**	111.68
11	75.39	39.05	**26**		85.03	**41**	113.29
12	77.23	43.27	**27**		85.81	**42**	119.07
13	88.56	45.11	**28**		89.32	**43**	123.56
14	91.21	49.50	**29**		90.20	**44**	126.89
15	96.63	51.99	**30**		91.90	**45**	129.06

It may be mentioned that (a) the Borrego Mountain motion has energy distributed in a broadband of 0.7–9.5 s and a dominant period of 5.65 s, (b) the El-Centro motion has energy distributed in a broadband of 0.2–3 s and a dominant period of 0.47 s, (c) the Kern County motion has energy distributed in a broadband of 0.2–7 s and a dominant period of 0.35 s, (d) the Michoacan motion has energy distributed in a narrowband of 1.6–3 s and a dominant period of 2 s, (e) the Parkfield motion has energy distributed in a narrowband of 0.25–0.6 s and a dominant period 0.28 s, (f) the San Fernando motion has energy distributed in a narrowband of 4–7 s and a dominant period of 5.65 s (Ghumadwar and Gupta, 2025).

Six ensembles of 259 ground motions each are generated corresponding to the seismic hazards represented by the 5%-damping PSA spectra of the six example ground motions by making a set of 259 recorded ground motions compatible with these PSA spectra as in Mukherjee and Gupta (2002). The set of 259 ground motions considered has been chosen by Saifullah and Gupta (2020) from the database of 1482 accelerograms recorded during the 106 earthquake events that occurred in the western region of U.S.A. between 1931 and 1984. The details regarding the database are given in Lee and Trifunac (1987). The chosen ground motions are characterized by peak ground acceleration (PGA) > $0.15g$, epicentral distance ranging from 4 to 62 km, earthquake magnitude ranging from 4.5 to 6.9, and T_s (as defined in Trifunac and Brady (1975)) ranging from 1.8 to 42 s. It may be noted that the motions in each of the six ensembles generated are compatible with the same 5%-damping PSA spectrum, which varies from ensemble to ensemble.

2. Computation of Actual and Estimated Peak Responses

Each of the five example buildings is subjected to the (spectrum-compatible) ground motions of the six ensembles (in the x-direction for BD4 and BD5), and the peak response of a floor/story is obtained for a building-ensemble combination by averaging the peak responses obtained for that floor/story from the time-history analyses of the building under the excitation of the 259 motions of the ensemble. Thus, a total of 66 values of peak floor displacements or peak story shears are obtained (which are in the x-direction for BD4 and BD5) for each of the six seismic hazards, where a seismic hazard is represented by the 5%-damping PSA spectrum averaged over the 259 motions of the corresponding ensemble. Let the value of a peak floor/story response under a seismic hazard be denoted by $(r_{\text{peak}})^{\text{act}}$.

For the estimated value $(r_{\text{peak}})^{\text{est}}$ of the peak floor/story response, the input spectrum data to the modal combination rule in Equation (1) is obtained by averaging the 5%-damping SD and SV spectra over the set of 259 (spectrum-compatible) motions of the ensemble for the seismic hazard under consideration. Further, the input normalized modal peak factors (i.e., $\bar{p}_j^D$, $\bar{p}_j^V$, $j = 1, 2, \ldots, n$) are obtained by averaging the 259 actual values of these peak factors determined for the set of 259 motions of the ensemble, where

the actual values of these peak factors for the jth mode are obtained for an ensemble motion by computing the nonstationary peak factors p_G, p_j^D, and p_j^V as in Equations (9), (10), and (11), respectively, for the oscillator of ω_j frequency and ζ_j damping ratio, and then by normalizing the so-obtained p_j^D and p_j^V values with respect to the p_G value. These input spectrum and peak factor data are now used in Equation (23) for a given value of q to obtain the normalized peak factor $\bar{p}_r$ for the response $r(t)$ being considered. Finally, the peak floor/story response $(r_{\text{peak}})^{\text{est}}$ is estimated (using Equation (1)) to give 66 values of peak floor displacements or peak story shears for a seismic hazard and q value. These calculations are carried out for different values of the parameter q, considered at the interval of 0.1 in the 1–5 range, to arrive at the optimum values of q for the floor displacement and story shear responses.

3. Optimum Values of q

For a given value of q, the error associated with the estimated peak value $(r_{\text{peak}})^{\text{est}}$ is determined by comparing it with the actual peak value $(r_{\text{peak}})^{\text{act}}$ for all the 396 combinations of floor/story and seismic hazard in the cases of floor displacement and story shear responses, and those 396 error values are used to determine the RMS error in each of these cases as

$$e = \left[\sum_{1}^{396} \left\{ \frac{(r_{\text{peak}})^{\text{act}} - (r_{\text{peak}})^{\text{est}}}{(r_{\text{peak}})^{\text{act}}} \times 100 \right\}^2 \Big/ 396 \right]^{\frac{1}{2}} \tag{24}$$

The values of the RMS error e are determined for all the q values considered, and the variation of e with the parameter q is plotted for each of the two response cases (i.e., floor displacement and story shear). For a response case, the value of q at which the RMS error e is minimized is considered to be the optimum value of q for use in Equation (23).

Figures 1(a) and 1(b) show the variations of the RMS error e with q for the response cases of floor displacement and story shear, respectively. These figures give the optimum values of q as 2.4 for the floor displacement response (with the RMS error of 2.3%), and 1.8 for the story shear response (with the RMS error of 16.65%). It may be noted that these values may have to be revised, if the damping ratio is uniformly not equal to 5% in all the modes of the building.

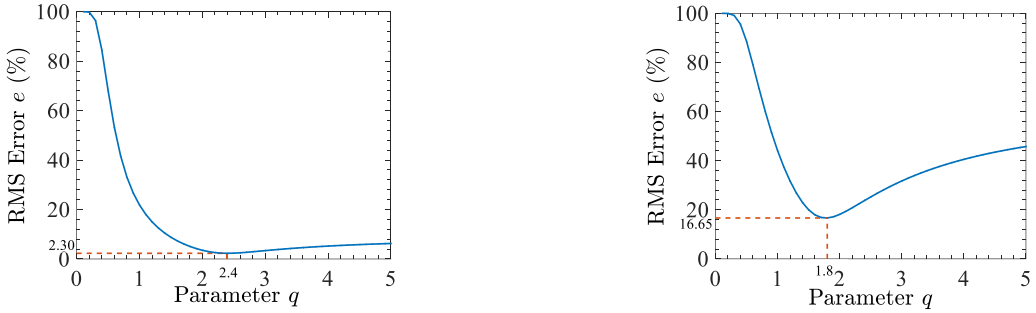

Fig. 1 Variation of RMS Error e in (a) Peak Floor Displacement Estimation and (b) Peak Story Shear Estimation, with Parameter q (with the optimum values of q and corresponding RMS errors indicated)

ILLUSTRATION OF PROPOSED MODAL COMBINATION RULE

It will be useful to illustrate the performance of the modal combination rule described in Equation (1) for the 30 combinations of example buildings (BD1 to BD5) and 5%-damping PSA spectra (obtained from averaging over the 259 motions of the ensembles corresponding to the Borrego Mountain, Imperial Valley, Kern County, Michoacan, Parkfield, and San Fernando motions). This is so because these rules are expected to use the modelled values of the normalized modal peak factors and SV ordinates (instead

of their actual values averaged over the ensemble) together with $\bar{p}_r$ estimated using Equation (23) and q taken as 2.4 or 1.8 (depending on whether the response is floor displacement or story shear). To this end, the modelled value of the displacement peak factor $\bar{p}_j^D$ is obtained as proposed by Ghumadwar and Gupta (2025), and the modelled value of the velocity peak factor $\bar{p}_j^V$ is taken as in Pal and Gupta (2021a). Further, the modelled SV ordinates, SV_j, for the natural frequency ω_j are taken as in Pal and Gupta (2021b).

The computed values of peak floor displacements and peak story shears for the 66 floors/stories under each of the six seismic hazards are compared with the $(r_{\text{peak}})^{\text{act}}$ values determined above. Figures 2(a) and 2(b) respectively show the cumulative distributions of percentage error and absolute percentage error in the peak floor displacement estimation based on 396 such values. For comparison, the error distributions are also shown for the conventional estimates obtained by using unity peak factors instead of the modelled peak factors. Figures 3(a) and 3(b) show such comparisons in respect of peak story shear estimation. It may be observed from both sets of figures that the use of modelled peak factors fails to improve upon the performance of the conventional approach. In the case of peak floor displacement estimation, up to the error level of about 14% for about 94% cases, the probability of the absolute error being below a given level is almost same for the two types of estimates, and there are about 3% cases, in which the modelled peak factors lead to larger absolute errors compared to the maximum error obtained with the conventional approach. In the case of peak story shear estimation, the modelled peak factors perform slightly better only for the absolute errors below 4% (for about 35% cases), and there are about 12% cases that have larger absolute errors with the use of modelled peak factors in comparison with the maximum absolute error for the conventional estimates.

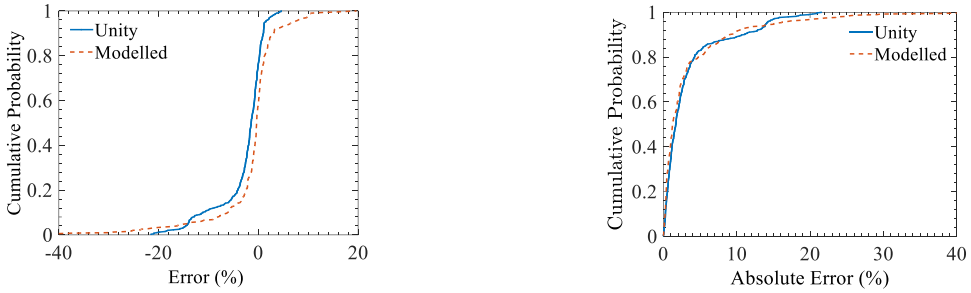

Fig. 2 Comparisons of Cumulative Distributions of (a) Percentage Error and (b) Absolute Percentage Error in Peak Floor Displacement Estimation by Using Unity and Modelled Peak Factors

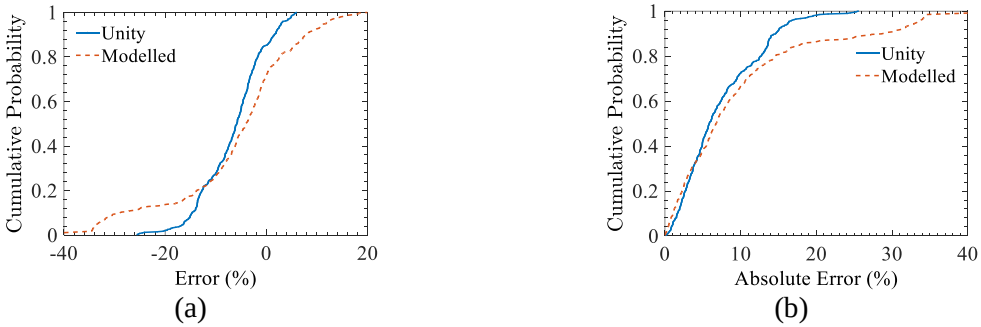

Fig. 3 Comparisons of Cumulative Distributions of (a) Percentage Error and (b) Absolute Percentage Error in Peak Story Shear Estimation by Using Unity and Modelled Peak Factors

The above illustration of the use of modelled peak factors in the modal combination rule of Equation (1) has shown that the errors in modelled peak factors may lead to large errors in the peak response estimation in a few cases. In order to avoid such extreme cases, it is proposed as in Pal and Gupta (2021a) to consider the conventional estimates based on unity peak factors instead, as and when the estimates based on the modelled peak factors deviate from those by more than 15%. Figure 4(a) shows the comparison of the revised absolute error distribution for the use of modelled peak factors (denoted by 'Modelled-Revised') with the 'Unity' and 'Modelled' distributions shown in Figure 2(b) in the case of

peak floor displacement estimation. Figure 4(b) shows similar comparison in the estimation of peak story shear. In Figure 4(a), it may be observed that the proposed modification reduces the extent of errors in the extreme cases of peak floor displacement estimation. Similarly, Figure 4(b) shows in the case of peak story shear estimation that the performance of Equation (1) with the use of modelled peak factors becomes almost as good as that of the conventional approach (of unity peak factors) due to the proposed modification.

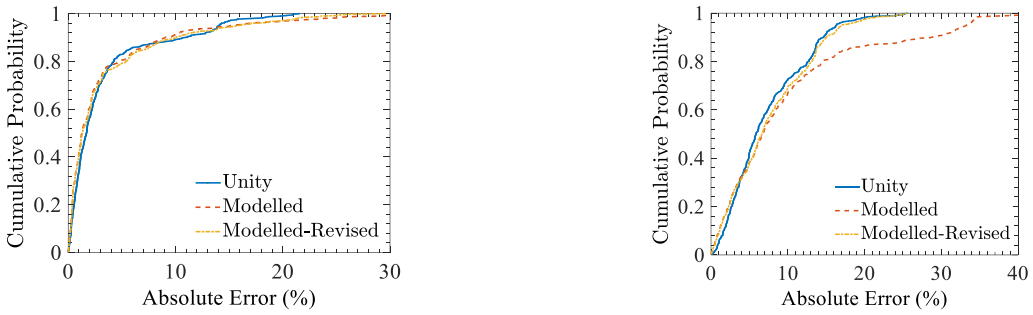

Fig. 4 Comparisons of Cumulative Distributions of Absolute Percentage Error in (a) Peak Floor Displacement Estimation and (b) Peak Story Shear Estimation, by Using Unity, Modelled, and Modelled-Revised Peak Factors

The results given in Figures 2–4 have been based on the same ensembles of ground motions as those used for the calibration of q. It will therefore be desirable to illustrate the use of modelled peak factors in the modal combination rule of Equation (1), together with the proposed modification for the extreme cases, by considering entirely different ensembles of ground motions. To this end, four new ensembles of 100 spectrum-compatible ground motions each are considered instead of the six ensembles of 259 spectrum-compatible motions each. These ensembles are same as those considered by Ghumadwar and Gupta (2025) and are generated by making 100 recorded motions compatible with the 5%-damping PSA spectra of the four recorded ground motions listed in Table 7. The 66 actual values of each of the peak responses (i.e., floor displacement and story shear) are obtained for each of the four example motions by averaging the time-history analysis estimates of the peak response for the corresponding ensemble of 100 spectrum-compatible motions, whereas the estimates of that peak response from the modal combination rule of Equation (1) (for the hazard represented by the same example motion) are obtained by using (a) the PSA spectrum obtained by averaging the 5%-damping PSA spectra of the 100 spectrum-compatible motions, and (b) the modelled values of the 5%-damping SV spectrum and various normalized peak factors. The estimates from the modal combination rule are also obtained for the cases of (a) various normalized peak factors assumed to be unity, and (b) proposed modification with the use of modelled peak factors.

Table 7: Details of ground motions considered to generate four ensembles of 100 spectrum-compatible motions each (for the illustration of the proposed modal combination rule)

S. No.	Name of Earthquake	Recording Site Location	Component
1	2006 Kiholo Bay Earthquake	Kona Hospital, Kealakekua	North
2	2016 Amberley Earthquake	Molesworth Station	N77E
3	2016 Amberley Earthquake	Te Mara Farm, Waia	S62W
4	2015 Nepal Earthquake	Kanti Path, Kathmandu	North

Figures 5(a) and 5(b) respectively show the comparisons of the percentage error and absolute percentage error distributions in the peak floor displacement estimation under the ‘Unity’, ‘Modelled’, and ‘Modelled-Revised’ cases based on 264 data points each. Figures 6(a) and 6(b) show similar comparisons in the case of peak story shear estimation. It may be observed that for the new suite of ground motions, (a) errors obtained with the use of the modelled peak factors (see the ‘Modelled’ curve) are significantly reduced by applying the proposed modification for the extreme cases (see the ‘Modelled-Revised’ curve), and (b) the ‘Unity’ and ‘Modelled-Revised’ curves are quite close to each other, and thus the use of modelled peak factors together with the proposed modification works almost as well as the

conventional use of unity peak factors in Equation (1). This implies that the estimates based on the use of modelled peak factors (with the proposed modification for the extreme cases) are as accurate as those from the conventional approach (based on the use of unity peak factors) or better than those. Accordingly, it is proposed to use the modal combination rule given in Equation (1) together with the use of modelled or unity peak factors, depending on whether the estimates based on modelled peak factors deviate by more than 15% from the estimates based on unity peak factors.

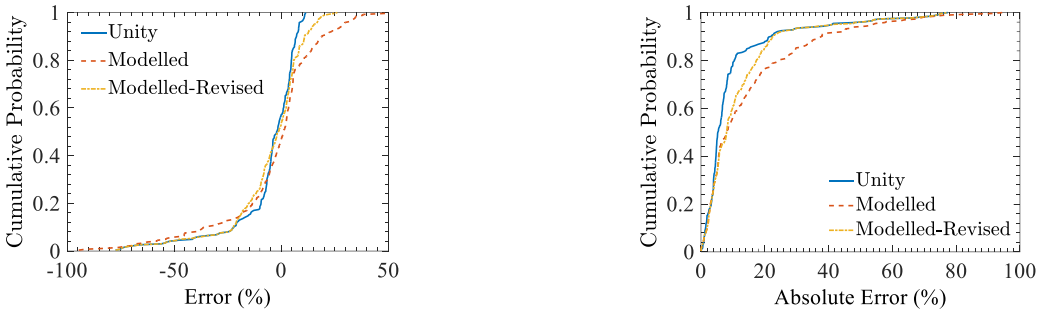

Fig. 5 Comparisons of Cumulative Distributions of (a) Percentage Error and (b) Absolute Percentage Error in Peak Floor Displacement Estimation by Using Unity, Modelled, and Modelled-Revised Peak Factors in Case of Four Ground Motion Ensembles Used for Illustration

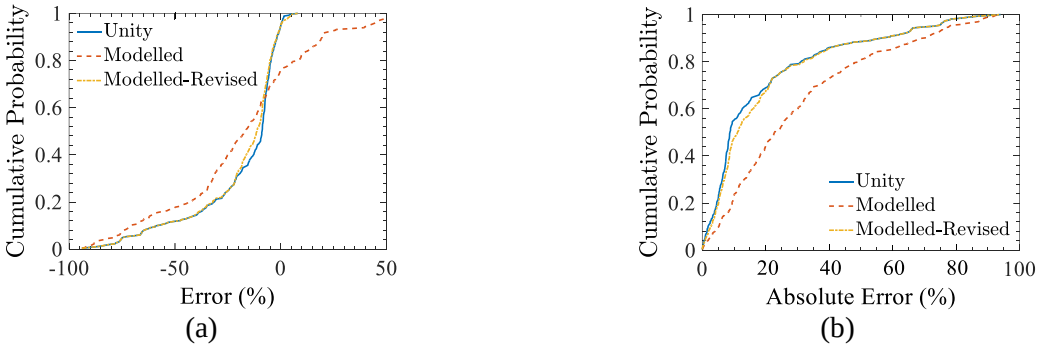

Fig. 6 Comparisons of Cumulative Distributions of (a) Percentage Error and (b) Absolute Percentage Error in Peak Story Shear Estimation by Using Unity, Modelled, and Modelled-Revised Peak Factors in Case of Four Ground Motion Ensembles Used for Illustration

COMPARISON WITH EXISTING MODAL COMBINATION RULES

A comparative study is carried out to illustrate the performance of the proposed modal combination rule vis-à-vis the existing modal combination rules for peak floor displacement and peak story shear. To this end, the 30 combinations of five example buildings (BD1 to BD5) and six seismic hazard cases (represented by the Borrego Mountain, Imperial Valley, Kern County, Michoacan, Parkfield, and San Fernando motions) are considered, and thus there is no change in the averaged time-history analysis results and the input data for the modal combination rules as obtained above. All the 30 combinations lead to a total of 396 actual or estimated values of peak floor displacement or peak story shear, where the estimated values correspond to (a) the proposed approach, (b) the modal combination rule in Equation (1) using unity peak factors (with the SV ordinates modelled as in the proposed rule), (c) the PSDF-based Category III method of Gupta (2002), and (d) the CSRSS rule proposed by Heredia-Zavoni (2011) (with the Kanai-Tajimi PSDF-based calculation of characteristic frequency).

1. Peak Floor Displacement

The cumulative distributions of percentage error and absolute percentage error obtained for the four approaches are compared in Figures 7(a) and 7(b) respectively. The cumulative distribution for the proposed approach (denoted by ‘P’) in Figure 7(a) is identical to the ‘Modelled-Revised’ curve in Figure 4(a), while that for the rule in Equation (1) using unity peak factors (denoted by ‘C1’) is identical to the ‘Unity’ curve. Even though the PSDF-based methods of Gupta (2002) and Heredia-Zavoni (2011)

do not enjoy the simplicity and convenience of modal combination rules (because both methods do not solely use the spectrum ordinates) and thus cannot be compared with a modal combination rule, the estimates from the two methods are expected to be more accurate and are thus included in order to provide a perspective to the usefulness of the proposed modal combination rule.

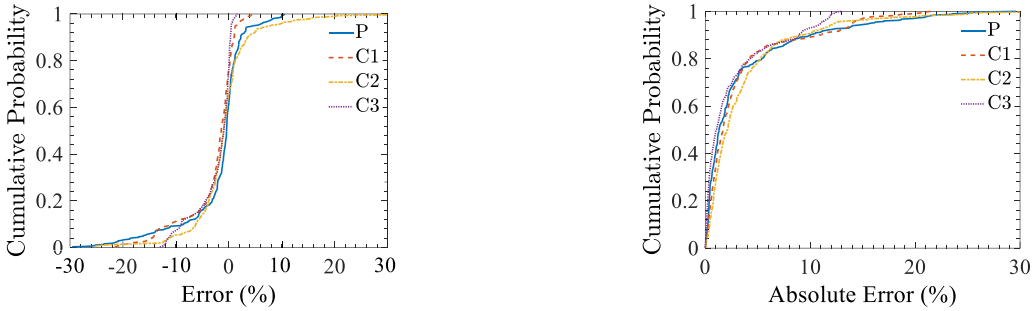

Fig. 7 Comparisons of Cumulative Distributions of (a) Percentage Error and (b) Absolute Percentage Error in Peak Floor Displacement Estimation by Proposed Rule (P), Rule in Equation (1) with Unity Peak Factors (C1), CSRSS Rule (C2), and PSDF-Based Method of Gupta (C3)

It may be observed in Figure 7(b) that the performance of the PSDF-based method of Gupta (2002) is superior to the performances of the other methods, and that the performance of the proposed rule falls below this performance primarily in respect of the maximum absolute error. Whereas this error is 13% for the PSDF-based method of Gupta (2002), it becomes 30% for the proposed rule. The cumulative distributions for the two methods are reasonably close for the errors up to 9%, which accounts for about 88% cases. As shown by Figure 7(a), both methods are also associated with a greater probability of underestimation.

The comparison of the four (approximate) approaches in respect of the absolute percentage error averaged over all the floors of a building under a seismic hazard is shown in Table 8 for each of the 30 combinations of buildings and seismic hazards. The largest average error among these combinations for

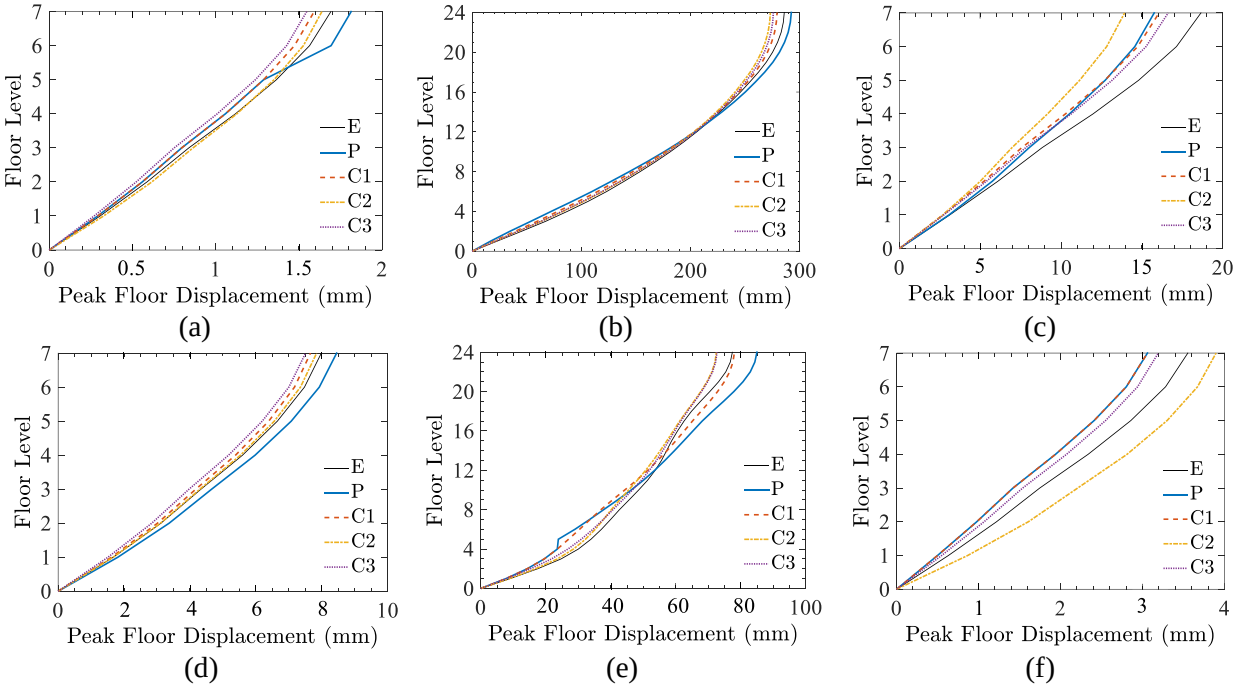

Fig. 8 Comparisons of Exact (E) Peak Floor Displacement Envelopes with Estimated Envelopes from Proposed Rule (P), Rule in Equation (1) with Unity Peak Factors (C1), CSRSS Rule (C2), and PSDF-Based Method of Gupta (C3) in (a) BD4 and Borrego Mountain, (b) BD1 and Imperial Valley, (c) BD4 and Kern County, (d) BD4 and Michoacan, (e) BD1 and Parkfield, and (f) BD4 and San Fernando Combinations

Table 8: Comparison of averaged absolute percentage errors in peak floor displacement estimates from four different approximate methods for 30 combinations of example buildings and seismic hazards

Approximate Method	Example Motion					
	Borrego Mountain	**Imperial Valley**	**Kern County**	**Michoacan**	**Parkfield**	**San Fernando**
	Example Building BD1					
Proposed	2.33	**6.61**	8.62	0.27	**11.23**	1.37
Unity Peak Factors	2.18	4.07	5.96	1.19	8.47	0.88
CSRSS	1.57	3.18	4.92	0.93	4.53	5.04
PSDF Method of Gupta	1.26	2.88	4.87	0.44	5.36	0.90
	Example Building BD2					
Proposed	0.56	0.83	0.60	2.15	3.24	0.20
Unity Peak Factors	0.76	1.78	0.56	2.88	2.10	0.87
CSRSS	0.94	1.49	0.84	1.64	3.90	4.76
PSDF Method of Gupta	0.28	0.87	0.48	1.12	1.76	0.51
	Example Building BD3					
Proposed	1.36	0.33	0.70	2.27	1.33	0.66
Unity Peak Factors	0.72	0.40	0.76	2.57	0.97	1.14
CSRSS	1.09	0.40	0.56	2.36	0.70	4.07
PSDF Method of Gupta	0.64	0.28	0.10	1.29	0.29	0.63
	Example Building BD4					
Proposed	**5.85**	6.21	**10.43**	**6.95**	5.48	**<u>17.23</u>**
Unity Peak Factors	5.32	12.63	14.07	3.74	9.39	<u>17.23</u>
CSRSS	3.16	10.76	21.63	1.06	12.06	<u>21.85</u>
PSDF Method of Gupta	9.95	9.21	11.31	7.67	<u>11.68</u>	11.43
	Example Building BD5					
Proposed	1.04	0.77	1.98	0.80	3.94	0.34
Unity Peak Factors	1.30	1.49	1.72	2.02	3.23	1.23
CSRSS	1.47	1.06	2.25	1.36	4.11	5.82
PSDF Method of Gupta	0.55	0.66	1.34	1.45	3.36	0.78

Note: Underlined values denote the largest average error (among the 30 combinations of example buildings and hazards) for each method. Bold values denote the largest average error (among the five example buildings) for the proposed rule under each seismic hazard.

each approach is underlined. The values shown in bold represent the largest average errors (over the five example buildings) for the six seismic hazards in the case of the proposed rule. It may be observed that the largest average error is obtained as 17.23% for both proposed rule and the rule in Equation (1) with unity peak factors (in the case of BD4 building under the seismic hazard of the San Fernando motion) in comparison with the lowest value of 11.68% for the PSDF-based method of Gupta (2002) (in the case of BD4 building under the seismic hazard of the Parkfield motion). Further, there are three cases (out of a total of 30 cases), in which the average error exceeds 10% for these three approaches. This indicates that the proposed rule for peak floor displacement does not sacrifice significantly on the accuracy of estimation in comparison with the PSDF-based method of Gupta (2002) despite avoiding the computational effort involving PSDF.

The envelopes of peak floor displacement estimates from the four approaches are compared in Figures 8(a)–8(f) with the (exact) time-history envelopes for an illustration of the relative performance of the proposed rule. These envelopes correspond to the critical cases for the proposed approach (in respect of the largest average error) under the seismic hazards of Borrego Mountain, Imperial Valley, Kern County, Michoacan, Parkfield, and San Fernando motions, respectively, and are for the buildings BD4, BD1, BD4, BD4, BD1, and BD4, respectively. It may be observed that the envelopes obtained from the proposed rule consistently underestimate the exact envelopes in the cases of Kern County and San Fernando motions (see Figures 8(c) and 8(f)) and that these envelopes overestimate or fluctuate around the exact envelopes in the remaining four cases. This appears to be a reasonable performance considering that the envelopes from the PSDF-based method of Gupta (2002) underestimate the exact envelopes in all the six cases and the envelopes from the rule in Equation (1) with unity peak factors underestimate in five of the six cases.

2. Peak Story Shear

Figures 9(a) and 9(b) compare the cumulative distributions of percentage error and absolute percentage error corresponding to the four approaches. The cumulative distributions in Figure 9(a) for the proposed rule and the rule in Equation (1) with unity peak factors respectively are identical to the 'Modelled-Revised' and 'Unity' curves in Figure 4(b). Table 9 gives the absolute percentage errors averaged over all the stories of a building for each of the 30 combinations of buildings and seismic hazards in the case of all the four approaches (the underlined values indicate the overall largest errors for the four approaches, and the values shown in bold indicate the largest errors determined across different buildings for different seismic hazards in the case of the proposed rule). Finally, Figures 10(a)–10(f) show the envelopes of peak story shear estimates obtained from the four approaches together with the (exact) time-history envelopes for the building-hazard combinations corresponding to the values shown in bold in Table 9. These critical cases (for the proposed approach) correspond to the BD1-Borrego Mountain, BD1-Imperial Valley, BD1-Kern County, BD4-Michoacan, BD1-Parkfield, and BD4-San Fernando combinations of building and seismic hazard, respectively.

The performance of the PSDF-based method of Gupta (2002) is seen to be superior to the performances of the other approaches in Figure 9(b), primarily because the maximum absolute error is 19% for this approach as compared to 26% for the proposed rule and the rule in Equation (1) with unity peak factors, and 88% for the CSRSS rule. For the absolute errors up to 14% which accounts for about 90% cases, the cumulative distribution for the proposed rule is quite close to that for the PSDF-based method of Gupta (2002), and thus the proposed rule does not compromise significantly on accuracy due to the simplifications incorporated. Further, as shown by Figure 9(a), most of the estimates from the two

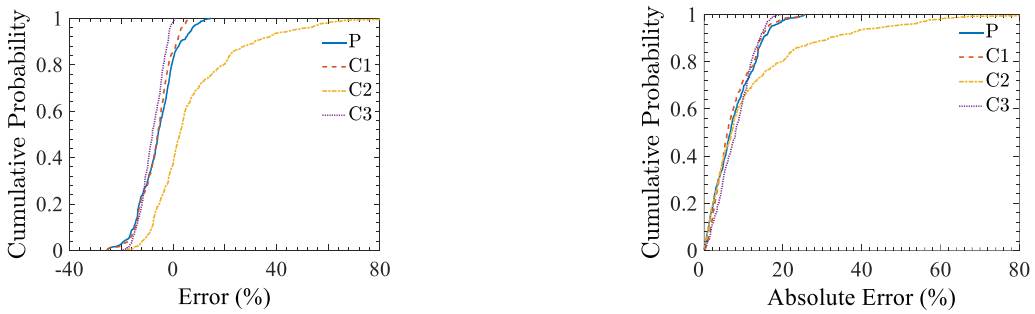

(a) (b)

Fig. 9 Comparisons of Cumulative Distributions of (a) Percentage Error and (b) Absolute Percentage Error in Peak Story Shear Estimation by Proposed Rule (P), Rule in Equation (1) with Unity Peak Factors (C1), CSRSS Rule (C2), and PSDF-Based Method of Gupta (C3)

Table 9: Comparison of averaged absolute percentage errors in peak story shear estimates from four different approximate methods for 30 combinations of example buildings and seismic hazards

Approximate Method	Example Motion					
	Borrego Mountain	**Imperial Valley**	**Kern County**	**Michoacan**	**Parkfield**	**San Fernando**
	Example Building BD1					
Proposed	**12.59**	**13.12**	**14.98**	2.41	**8.31**	11.93
Unity Peak Factors	12.52	12.56	9.88	8.16	7.57	9.93
CSRSS	7.42	9.73	7.11	8.17	3.40	38.57
PSDF Method of Gupta	10.48	10.08	8.00	3.46	9.66	8.56
	Example Building BD2					
Proposed	2.86	4.56	6.35	4.80	5.78	7.50
Unity Peak Factors	4.82	4.22	2.86	7.73	2.58	10.57
CSRSS	10.78	3.84	9.38	2.75	4.49	35.74
PSDF Method of Gupta	6.77	5.34	5.66	8.37	3.86	8.55
	Example Building BD3					
Proposed	7.48	0.66	2.10	3.03	5.79	7.19
Unity Peak Factors	1.16	3.57	3.96	2.92	2.47	8.94
CSRSS	6.93	2.36	5.44	1.17	1.64	28.29
PSDF Method of Gupta	5.52	4.19	3.50	6.16	1.82	5.20
	Example Building BD4					
Proposed	5.96	4.47	10.35	**7.00**	5.96	**23.65**
Unity Peak Factors	3.84	7.92	12.12	2.79	3.84	23.65
CSRSS	12.99	9.83	16.57	0.57	10.68	54.87
PSDF Method of Gupta	15.32	14.36	14.94	11.69	12.07	16.32
	Example Building BD5					
Proposed	2.90	7.09	5.88	2.98	4.52	10.03
Unity Peak Factors	5.24	1.93	1.87	6.63	2.28	13.05
CSRSS	11.74	4.64	9.66	6.54	4.83	36.32
PSDF Method of Gupta	7.10	6.75	6.20	8.70	5.26	9.81

Note: Underlined values denote the largest average error (among the 30 combinations of example buildings and hazards) for each method. Bold values denote the largest average error (among the five example buildings) for the proposed rule under each seismic hazard.

approaches are on the non-conservative side. On considering the averaged absolute percentage errors shown in Table 9, it may be observed that both the proposed rule and the rule in Equation (1) with unity peak factors lead to the maximum error of 23.65% as compared to the error of 16.32% in the case of the PSDF-based method of Gupta (2002) (for the BD4 building under the San Fernando motion). Also, there are comparable number of cases (6 in the case of the rule in Equation (1) with unity peak factors, 7 in the case of the proposed rule, and 8 in the case of the PSDF-based method of Gupta (2002)), which are associated with the averaged error exceeding 10%. Thus, the performance of the proposed rule compares well with the more involved and accurate PSDF-based method of Gupta (2002) for peak story shear estimation as well. Also, as observed from the envelopes shown in Figures 10(a)–10(f), the envelopes obtained from the proposed rule follow the exact envelopes well, just like the envelopes obtained from the PSDF-based method of Gupta (2002).

SUMMARY AND CONCLUSIONS

The response spectrum-based modal combination rule proposed by Gupta (1996) to estimate the largest peak amplitude of the linear response of a lumped mass, classically damped, multistoried structure, which is subjected to ground acceleration at its base, has been modified to include the role of normalized nonstationary peak factors (where normalization is with respect to the nonstationary peak factor for ground acceleration). This rule specifically considers those overall responses that can be expressed as a linear combination of the floor displacements of the structure, e.g., the relative floor displacement and story shear responses. The spectral amplitudes required for this formulation are the SD and SV amplitudes corresponding to the specified seismic hazard (in terms of the PSA amplitudes). The proposed rule uses the approximation of SV amplitudes (from the specified (design) PSA spectrum) as in Pal and Gupta (2021b). The proposed rule also uses the normalized nonstationary peak factors proposed by Ghumadwar and Gupta (2025) and Pal and Gupta (2021a) respectively for the relative displacement and relative velocity responses of base-excited SDOF oscillators.

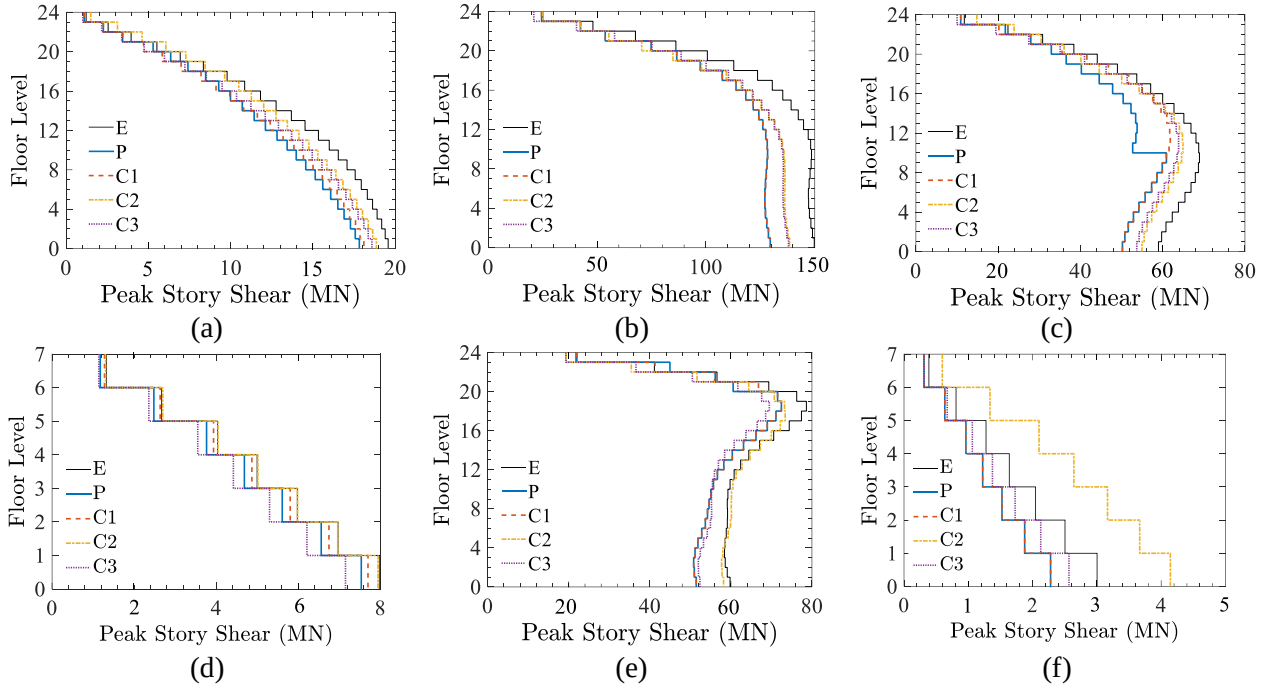

Fig. 10 Comparison of Exact (E) Peak Story Shear Envelopes with Estimated Envelopes from Proposed Rule (P), Rule in Equation (1) with Unity Peak Factors (C1), CSRSS Rule (C2), and PSDF-Based Method of Gupta (C3) in (a) BD1 and Borrego Mountain, (b) BD1 and Imperial Valley, (c) BD1 and Kern County, (d) BD4 and Michoacan, (e) BD1 and Parkfield, and (f) BD4 and San Fernando Combinations

The normalized nonstationary peak factor for the overall response has been modelled by first formulating the peak factor for the case of negligible cross-modal correlation and then by generalizing the so-obtained expression through a parameter q to account for non-negligible correlation. The proposed expression is in terms of (a) the (normalized) peak factors for different modal responses contributing to the structural response, and (b) the weights measuring the relative contributions of different modes to the peak factor for the overall response. The proposed peak factor model has been calibrated (through the determination of the parameter q) based on the actual peak factors computed from the time-history analysis estimates of peak floor displacements and peak story shears in the case of five example buildings and six ground motion ensembles.

The proposed modal combination rule envisages various normalized peak factors to be uniformly taken as unity as in the conventional approach, in case the estimates based on using the peak factor models show large deviations from those based on the unity peak factors. This has been done to avoid large errors in peak response estimation due to the errors inherent in the modelling of normalized peak factors. An illustration of the proposed modal combination rule based on four ensembles of ground

motions and five example buildings shows that the estimates from this rule are at least as accurate as those based on the use of unity peak factors.

A comparative study based on six different ensembles of ground motions (and same five example buildings) shows that the proposed modal combination rule gives almost as accurate peak response estimates as the rules based on the calculation of moments from the PSDF of ground motion. In the case of peak floor displacements, there is 88% probability with the proposed rule that the absolute error would be less than 9%, which is also the case for the PSDF-based estimates. Similarly, there is 10% probability for both methods that the averaged absolute error would exceed 10%. In the case of peak story shears, there is 90% probability with the proposed rule as well as the PSDF-based approach that the absolute error would be less than 14%. Further, there are about 25% cases for the two approaches in which the averaged absolute error exceeds 10%. Thus, the proposed modal combination rule does not compromise significantly on the accuracy of estimation in comparison with the PSDF-based methods, while avoiding the complexity and computational effort inherent with the use of ground motion PSDF consistent with the specified seismic hazard. Further, since the conventional version of the proposed rule delivers a similar performance vis-à-vis the PSDF-based methods, this may be an attractive alternative due to its simplicity.

REFERENCES

1. Anagnostopoulos, S.A. (1982). "Wave and Earthquake Response of Offshore Structures: Evaluation of Modal Solutions", *Journal of the Structural Division, Proceedings of ASCE,* Vol. 108, No. ST10, pp. 2175–2191.
2. Biot, M.A. (1943). "Analytical and Experimental Methods in Engineering Seismology', *ASCE Transactions,* Vol. 108, No. 1, pp. 365–385.
3. Chopra, A.K. (2021). "Modal Combination Rules in Response Spectrum Analysis: Early History", *Earthquake Engineering & Structural Dynamics,* Vol. 50, No. 2, pp. 260–269.
4. Der Kiureghian, A. (1981). "A Response Spectrum Method for Random Vibration Analysis of MDF Systems", *Earthquake Engineering & Structural Dynamics,* Vol. 9, No. 5, pp. 419–435.
5. Der Kiureghian, A. and Nakamura, Y. (1993). "CQC Modal Combination Rule for High-Frequency Modes", *Earthquake Engineering & Structural Dynamics,* Vol. 22, No. 11, pp. 943–956.
6. Ghumadwar, A.S. and Gupta, V.K. (2025). "Use of Peak Factors in Response Spectrum-Based Modal Combination Rules for Peak Floor Accelerations", *Journal of Engineering Mechanics, ASCE,* Vol. 151, No. 7, Paper 04025024.
7. Goodman, L.E., Rosenblueth, E. and Newmark, N.M. (1955). "Aseismic Design of Firmly Founded Elastic Structures", *Transactions of ASCE,* Vol. 120, No. 1, pp. 782–802.
8. Gupta, A.K. (1990). "Response Spectrum Method in Seismic Analysis and Design of Structures", *Blackwell Scientific Publications, Cambridge, U.S.A.*
9. Gupta, V.K. (1996). "A New Modal Combination Rule for the Building Response to Earthquakes", *Proceedings of International Seminar on Civil Engineering Practices in the Twentyfirst Century, Roorkee,* Vol. III, pp. 1756–1764.
10. Gupta, V.K. (2002). "Developments in Response Spectrum-Based Stochastic Response of Structural Systems", *ISET Journal of Earthquake Technology,* Vol. 39, No. 4, pp. 347–365.
11. Gupta, V.K. (2009). "A New Approximation for Spectral Velocity Ordinates at Short Periods", *Earthquake Engineering & Structural Dynamics,* Vol. 38, No. 7, pp. 941–949.
12. Gupta, I.D. (2018). "An Overview of Response Spectrum Superposition Methods for MDOF Structures" (in "Advances in Indian Earthquake Engineering and Seismology: Contributions in Honour of Jai Krishna", edited by M.L. Sharma, M. Shrikhande, and H.R. Wason), *Springer, Cham, Switzerland,* pp. 335–364.
13. Gupta, V.K. and Trifunac, M.D. (1990). "Response of Multistoried Buildings to Ground Translation and Rocking during Earthquakes", *Probabilistic Engineering Mechanics,* Vol. 5, No. 3, pp. 138–145.
14. Heredia-Zavoni, E. (2011). "The Complete SRSS Modal Combination Rule", *Earthquake Engineering & Structural Dynamics,* Vol. 40, No. 11, pp. 1181–1196.
15. Jennings, R.L. (1958). "The Response of Multi-Storied Structures to Strong Ground Motion", *M.Sc. Thesis, University of Illinois, Urbana, U.S.A.*

16. Lee, V.W. and Trifunac, M.D. (1987). "Strong Earthquake Ground Motion Data in EQINFOS: Part 1", *Report CE 87-01, University of Southern California, Los Angeles, U.S.A.*
17. Lindley, D.W. and Yow, J.R. (1980). "Modal Response Summation for Seismic Qualification", *Proceedings of ASCE Specialty Conference on Civil Engineering and Nuclear Power, Knoxville, U.S.A.*, Vol. VI, Paper No. 8-2, pp. 1–28.
18. Merchant, H.C. and Hudson, D.E. (1962). "Mode Superposition in Multi-Degree of Freedom Systems Using Earthquake Response Spectrum Data", *Bulletin of the Seismological Society of America*, Vol. 52, No. 2, pp. 405–416.
19. Mukherjee, S. and Gupta, V.K. (2002). "Wavelet-Based Generation of Spectrum-Compatible Time-Histories", *Soil Dynamics and Earthquake Engineering*, Vol. 22, No. 9–12, pp. 799–804.
20. O'Hara, G.J. and Cunnif, P.F. (1963). "Elements of Normal Mode Theory", *Report 6002, U.S. Naval Research Laboratory, Washington, D.C., U.S.A.*
21. Pal, A. and Gupta, V.K. (2021a). "Peak Factor-Based Modal Combination Rule of Response-Spectrum Method for Peak Floor Accelerations", *Journal of Structural Engineering, ASCE,* Vol. 147, No. 7, Paper 04021095.
22. Pal, A. and Gupta, V.K. (2021b). "A Note on Spectral Velocity Approximation at Shorter Intermediate Periods", *Soil Dynamics and Earthquake Engineering*, Vol. 141, Paper 106422.
23. Pathak, S. and Gupta, V.K. (2017). "On Nonstationarity-Related Errors in Modal Combination Rules of the Response Spectrum Method", *Journal of Sound and Vibration*, Vol. 407, pp. 106–127.
24. Rosenblueth, E. and Elorduy, J. (1969). "Responses of Linear Systems to Certain Transient Disturbances", *Proceedings of the Fourth World Conference on Earthquake Engineering, Santiago, Chile*, Vol. I, Session A-1, pp. 185–196.
25. Saifullah, M. and Gupta, V.K. (2020). "Normalized Residual Displacements for Bi-linear and Pinching Oscillators", *Journal of Structural Engineering, ASCE,* Vol. 146, No. 11, Paper 04020242.
26. Samdaria, N. and Gupta, V.K. (2018). "A New Model for Spectral Velocity Ordinates at Long Periods", *Earthquake Engineering & Structural Dynamics,* Vol. 47, No. 1, pp. 169–194.
27. Singh, M.P. and Maldonado, G.O. (1991). "An Improved Response Spectrum Method for Calculating Seismic Design Response. Part 1: Classically Damped Structures", *Earthquake Engineering & Structural Dynamics,* Vol. 20, No. 7, pp. 621–635.
28. Singh, M.P. and Mehta, K.B. (1983). "Seismic Design Response by an Alternative SRSS Rule", *Earthquake Engineering & Structural Dynamics,* Vol. 11, No. 6, pp. 771–783.
29. Trifunac, M.D. and Brady, A.G. (1975). "A Study on the Duration of Strong Earthquake Ground Motion", *Bulletin of the Seismological Society of America,* Vol. 65, No. 3, pp. 581–626.
30. USNRC (1976). "Combining Modal Responses and Spatial Components in Seismic Response Analysis", *Regulatory Guide 1.9.2, Revision 1, U.S. Nuclear Regulatory Commission, Washington, D.C., U.S.A.*
31. Wilson, E.L., Der Kiureghian, A. and Bayo, E.P. (1981). "A Replacement for the SRSS Method in Seismic Analysis", *Earthquake Engineering & Structural Dynamics,* Vol. 9, No. 2, pp. 187–192.